Egypt. J. Chem. **Vol. 65,** No. 11 pp. 19 - 28 (2022)

Egyptian Journal of Chemistry

http://ejchem.journals.ekb.eg/

High -k Green Polymer Nanocomposites Based on Polyvinyl Alcohol for Electrostatic Dissipation Applications

D. A. Wissa[1], A. A. Ward[2], S. A. Gad[1], N. N. Rozik[3], A. Nassar[1], S. L. Abd-El-Messieh[2], S. S. Ibrahim[4], Sh. A. Khairy [4]*

[1]Physics Research Institute, Solid State Physics Department, National Research Centre Dokki, Giza, Egypt
[2]Physics Research Institute, Microwave Physics and Dielectrics Department, National Research Centre, Dokki, Giza, Egypt
[3]Chemical Industries Research Institute, Polymers and Pigments Department, National Research Centre, Dokki, Giza, Egypt
[4]Physics Department, College of Science, Cairo University, Giza, Egypt

Abstract

Polyvinyl alcohol (PVA) as a green biodegradable polymeric matrix was chosen to fabricate high-k (high permittivity) polymer nanocomposites with good magnetic and electric properties to be used for electrostatic dissipation applications. PVA was doped with different concentration of magnetite (Fe_3O_4) nanoparticles and barium titanate ($BaTiO_3$) nanoparticles before and after treatment with ionic liquid (IL). The magnetic properties were investigated by vibrating sample magnetometer (VSM) and the obtained results revealed an improvement in such properties by the ionic liquid treatment of $BaTiO_3$. This finding widens the application scope of PVA nanocomposites to include electromagnetic purposes. Moreover, electrical properties including permittivity ε′, dielectric loss ε″ in addition to electrical conductivity σ were also studied. The dielectric properties were also enhanced after ionic liquid treatment. In addition, the values of conductivity σ was in the order ~ 10^{-7} S/cm which endorse using such nanocomposites for electrostatic dissipation applications.

Keywords; Poly vinyl alcohol (PVA). Magnetic nanoparticles (MNPs). Magnetic properties. Dielectric properties. Electrical conductivity.

1. Introduction

Magnetic nanoparticles (MNPs) have attracted great interest in many life applications because of its magnetic properties as well as size in nanoscale, biocompatibility, crystallinity and surface modification potential. Although there have been numerous notable advancements in the manufacturing of magnetic nanoparticles, maintaining their stability for extended periods of time without agglomeration or precipitation remains a challenge [1]. To overcome agglomeration and provide homogenous distribution as usual, layers of MNPs were coated with polymeric materials such as polyethylene glycol (PEG), poly methyl methacrylate (PMMA) and polyvinyl alcohol (PVA), in order to retain magnetic properties required for high potential application in multi fields [2]. Among the various types of synthetic polymers that can be used for coating MNPs, PVA has potential applications, due to its thermal stability, high mechanical performance, and excellent biocompatibility. So a novel approach was made to dielectric composite materials is the combination of polymer materials with fillers and forming capabilities with a ceramic material, characterized by a high dielectric constant to generate a tailor built composite [1-3]. The selection of suitable polymer matrix and the proper filler can lead to the fabrication of excellent composites with variable dielectric characteristics. Polymer and ceramic compounds / ferroelectric particles can typically be manufactured using the casting method techniques. Composite films are prepared by mixing an insulating polymer solution and nano-sized ferroelectric particles, and evaporating the polymer solution solvent. Many efforts have been done in the last years to investigate alternative high-permittivity (high-k) dielectrics that could replace SiO2 and SiON

*Corresponding author e-mail: khairysh53@gmail.com
Receive Date: 5 June 2022, Revise Date: 22 June 2022, Accept Date: 29 June 2022
DOI: 10.21608/EJCHEM.2022.142955.6242

as gate insulators in the metal–oxide–semiconductor (MOS) transistors. The higher dielectric constant provides higher gate capacitances with moderated thickness layers. In addition, high-k dielectrics as novel metal electrodes are demanded to replace the traditional polysilicon gate electrode that is to avoid the polysilicon depletion, boron penetration, and compatibility issues with high-k dielectrics [4]. The most common process to enhance the dielectric permittivity of a polymer is the dispersion of a high electrical permittivity ceramic powder such as barium titanate ($BaTiO_3$) or lead titanate ($PbTiO_3$) in the polymer to form a composite. In order to obtain a high value of dielectric permittivity, a large amount of fillers must be loaded. Another way to obtain high dielectric permittivity composites is to use conductive filler such as magnetite (Fe_3O_4) near its percolation threshold to produce the composites [5]. These composites are versatile could simply processed and shaped to be readily treated and molded into any shape to be utilized for wide range of electrical and electronic applications [5-6]. Many investigations on polymer dielectrics with good processing qualities have been conducted, and it has been discovered that low-polarity covalent dipoles yield a comparatively low dielectric constant [6]. Composites made by dispersing inorganic filler particles in a polymer binder have a wide range of applications due to the combination of specific properties of two classes of compounds and the possibility of a wide range of property adjustment due to changes in component ratio and inorganic filler size [7]. This research focused on the preparation and characterization of a multifunctional PVA nanocomposite. PVA was simply mixed via casting method with different concentrations of magnetite and barium titanate nanoparticles in addition to barium titanate treated with ionic liquid as well. The physical properties of the prepared nanocomposites such as electrical, magnetic properties were reported.

2. Experimental

2.1 Materials and Methods

The samples were prepared by casting method to form three different nanocomposites (NCPs).

Materials

Poly vinyl alcohol (PVA) with M.Wt about 1.15,000 was provided from Loba Chemie and used as received. Fe_3O_4 nanoparticles (NPs) were prepared as mentioned before [8]. Barium titnate $BaTiO_3$ (M.Wt 233.24) was supplied from Merck KGaA (Germany).

1- Preparation of PVA / Fe_3O_4 NCPs

1 gm of PVA was dissolved in 30 mL of distilled water by stirring continuously at 30°C for 3 h using a magnetic stirrer. Then contents varying at (2.5, 5, 7, 10, 15 and 20) wt% of Fe_3O_4 (NPs) were added to the PVA suspension and mixed using ultrasonic path for 1 h and mechanical stirred for 24 h to reach a homogeneous distribution. Finally, the solution was poured onto glass plates and dried at 60 °C in an oven for 24 h to form films.

2- Preparation of PVA / 10 wt% Fe_3O_4 / $BaTiO_3$ NCPs

1 gm of PVA was dissolved 30 mL of distilled water and stirred continuously at 30°C for 3 h using a magnetic stirrer. Then set a constant as 10 wt% Fe_3O_4 and different content at (2.5, 5, 7, 10, 15 and 20) wt% of $BaTiO_3$ then follow the steps above to form NCPs films.

3- Preparation of PVA / 10 wt% Fe_3O_4 / IL treated $BaTiO_3$ NCPs.

The ionic liquid was prepared as mentioned before [9] . After that, The reactive surface of $BaTiO_3$ NPs has been treated with Ionic liquid as mentioned before [9,10]. Then 1 gm of PVA was dissolved in 30 mL of distilled water and stirred continuously at 30°C for 3 h using a magnetic stirrer. Then set a constant as 10 wt% Fe_3O_4 and different content at (2.5, 5, 7, 10, 15 and 20) wt% of IL treated $BaTiO_3$, then follow the same steps to get NCPs.

3. Techniques

Vibrating sample magnetometer (VSM) model Lake Shore Model 7410, USA was used for the magnetic properties measurements. The system is equipped with a 10-inch electromagnet providing magnetic fields up to 3.1 T, accuracy = +/- 1%, maximum sample size = 1 in and variable temperature (CCR) = ~20 K to 450 K.

Dielectric measurements including the permittivity (dielectric constant) ε', loss factor tan δ and ac-resistance R_{ac} were measured at room temperature ~ 25 °C in a broad frequency range (0.1 Hz - 1 MHz). The measurement was computerized by interfacing the impedance analyzer with a personal PC through a cable type GPIB IEE488. A commercial interfacing and automation software program "Lab VIEW" was used for data acquisition. The error in ε' and tan δ amounts to ±1 % and ±3 %, respectively.

The temperature of the samples was controlled by a temperature regulator with (Pt 100) sensor. The error in temperature measurements amounts ± 0.5 °C.

4. Results and Discussion

4.1 VSM Measurements

The magnetic properties of the prepared novel nanocomposites that consist of PVA polymer as a matrix and Fe_3O_4, $BaTiO_3$, IL treated $BaTiO_3$ as dopants are characterized by using VSM technique at room temperature. The VSM analysis was carried out at room temperature and hysteresis loops are shown in Figure (1) and Figure (2). Figure (1) shows the hysteresis loop of the PVA / Fe_3O_4 NCPs at different concentration (5, 10, 15 and 20) wt% of Fe_3O_4 NPs. Besides, the values of saturation magnetization (M_S), remanent magnetization (M_r) and coercivity force (H_c) are tabulated in Table1. From the Table it is shown that M_s increases from 1.85 to 8.24 emu/g with increasing Fe_3O_4 content but beyond a certain point the value of magnetization saturates and attains a maximum value of magnetization and domain grows. The samples show super paramagnetic nature with increasing NCPs loading which implies the ability of the sample to retain a large fraction of the magnetic field when the driving field was removed. However, an overdose of NPs content may lead to agglomeration, which may impede its dispersion in the matrix and uniform distribution of its magnetic moment. The values of H_c decreased when the content of NPs increased, this is due to the presence of nonmagnetic components with magnetite but the coercivity value at higher concentration of nanoparticles increased, this is due to the presence of surface roughness of nanoparticles at high content and also with the formation of ferromagnetic clusters in the polymer matrix [11,12]. It is clear from the discussion that adding Fe_3O_4 to nanocomposites improves magnetic behavior and increases the material's sensitivity to changes in the external magnetic field, resulting in an increase in magnetic values [13,14]. The property of super paramagnetic behavior of the nanocomposite suggest that it can be responsive to alternating current magnetic fields of magnetic separation, particle adsorption, and design of smart magnetic devices.

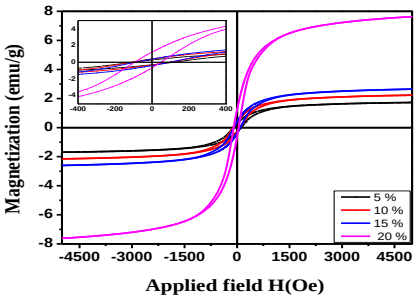

Figure (1): Hysteresis loop of PVA doped with (5, 10, 15 and 20) wt% of Fe_3O_4 NPs loading respectively.

Table1: Magnetic parameters of different content of Fe_3O_4 nanoparticles and copolymer nanocomposites

PVA / Fe_3O_4 Content (wt%)	**M_s (emu/g)**	**M_r (emu/g)**	**H_c (G)**
5	**1.85**	**0.29**	**108.94**
10	**2.37**	**0.36**	**102.90**
15	**2.84**	**0.44**	**103.88**
20	**8.24**	**1.35**	**104.85**

Figure (2) shows the hysteresis loop of the nanocomposites consisted of PVA / 10 wt% Fe_3O_4 / (5, 10, 15, 20) wt% $BaTiO_3$ and PVA / 10 wt% Fe_3O_4 / (5, 10, 15, 20) wt% IL treated $BaTiO_3$, the values of M_S, M_r and H_c with and without ionic liquid are tabulated in Table2. Figure (2) a, represents the hysteresis loops for PVA / 10 wt% Fe_3O_4 / $BaTiO_3$ NCPs at (5, 10, 15 and 20) wt% different content of $BatiO_3$, it showed that increase in M_s with increasing content of $BaTiO_3$ and also due to appearance of Fe_3O_4 with constant percent in NCPs. It showed that the composite material exhibits the typical ferromagnetic loops with super paramagnetic properties, also in the zoom curve that appear more broad hysteresis loop for high saturation indicate the NCP is more magnet [15]. Figure (2) b, represents the hysteresis loops for PVA /10 wt% Fe_3O_4 / IL treated $BaTiO_3$ NCPs at (5, 10, 15 and 20) wt% different content of treated, also clarified that the increment in M_s with increase content of IL treated $BaTiO_3$, may be due to the presence of a fixed ratio of Fe_3O_4 in NCPs, which helps the appearance of the super paramagnetic property. Also, the presence of IL with different content in NCPs improved the hysteresis loop shape, making it more regular and broader. So, we can explain that the presence of IL in the NCPs led to the improvement of magnetic properties and can be used in many electromagnetic applications [16].

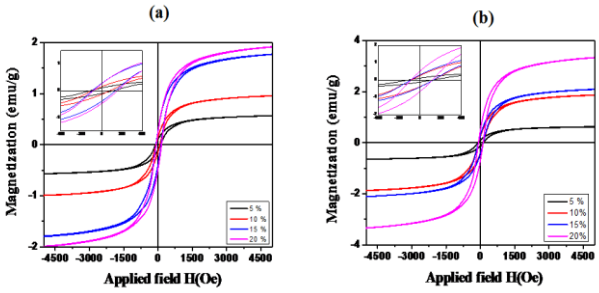

Figure (2): Hysteresis loop for (a) PVA / 10 wt% Fe_3O_4 doped with (5, 10, 15 and 20) wt% $BaTiO_3$ loading and (b) PVA /10 wt% Fe_3O_4 doped with (5 , 10, 15 and 20) wt% IL treated $BaTiO_3$ loading .

Table 2: Magnetic parameters of different content of $BaTiO_3$ and IL treated $BaTiO_3$ nanoparticles and copolymer nanocomposites

	Without treatment			Treated with ionic liquid		
PVA / 10 wt% Fe_3O_4 / $BaTiO_3$ Content (wt%)	M_s (emu/g)	M_r (emu/g)	H_c (G)	M_s (emu/g)	M_r (emu/g)	H_c (G)
5	0.62	0.11	112.93	0.69	0.12	118.18
10	1.06	0.18	111.22	2.03	0.33	110.76
15	1.92	0.31	104.98	2.27	0.35	107.60
20	2.11	0.34	107.63	3.61	0.61	105.82

4.2 Dielectric Measurements

The ability of polymers to store/ dissipate energy described by the terms permittivity (ε′) and dielectric loss (ε″). Both parameters are significantly affected by the polymer polarity, kind of filler, and loading amount. Figure (3) presents the variation of both ε′ and ε″ versus *f*, the applied frequency (10^{-1} -10^6 Hz) at room temperature (RT) ≅ 25°C. The permittivity ε′ of the NCPs was found to increase by increasing Fe_3O_4 and decrease shapely by increasing the applied frequency. The presence of Fe_3O_4 with its ionic dipoles masses could be the reason of the increase in ε′ values [17]. So a pronounced increase in ε′ values was detected as the result of increasing the content of the semiconductor Fe_3O_4 particles in the NCPs [18]. The high values of ε′ which were detected at low frequency could be owing to the compatibility of the interfacial electric dipoles and the electrical field at that range frequency so that the dipoles at the interface has strong ability to ordination at that low frequency [17].

The dielectric loss ε″ dependence upon the frequency, *f*, of PVA / Fe_3O_4 NCPs shown in Figure (3) reveals sharp decrease in ε″ by increasing the applied frequency up till ≅ 10^3 Hz after which an increase in ε″ values was detected. The dielectric loss ε″ is closely connected to the NCPs relaxation phenomena that measure the exponential decay of polarization with respect to time. The reduction in dielectric loss with increasing frequency is attributed to a variety of losses, including losses owing to dielectric non-uniformity, losses related to electrical conductivity, and Fe_3O_4 / PVA structure development [19]. The greater ε″ value in the low frequency range is due to free charge mobility inside the materials. In both instances, ε″ values increase by increasing Fe_3O_4 in the matrix. Anyway, the curves ε″ versus *f* are very complicated reflecting more than one relaxation manner [20,21]. These relaxation peaks are caused by the flexible side group or, in certain cases, by the mobility of the main chains and its correlated motions. For high performance energy storage application, the balance between high ε′ and low ε″ was demanded [22]. Curves relating both ε′ and ε″ at fixed *f* =100 versus Fe_3O_4, Figure (3) can reflect the feature of both ε′ and ε″. From this figure it is notable that the optimum content suitable for such application was 10 wt% of Fe_3O_4 after that concentration a dramatic increase in ε″ was detected.

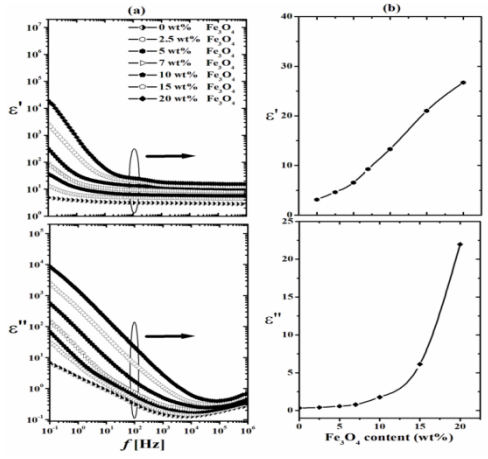

Figure (3): (a) ε′ and ε″ versus *f* for PVA/ Fe_3O_4 and both values versus Fe_3O_4 at fixed *f* = 100 Hz presented in (b) at room temperature (RT).

Cole–Cole plots aim to analyze the contribution of the relaxation mechanisms. The Nyquist diagram in Figure (4) shows the electric modulus complex smooth plots (Cole–Cole plots), M'' vs. M' (imaginary part vs. real part of the electric modulus)

for PVA / Fe_3O_4. At this temperature, the Cole–Cole plots reveal two arcs. The first one relates to lower frequency, i.e., left side semicircle, is a result of crankshaft types of motion of the main polymeric chain in which a few segments are involved (αβ). Whereas, the second relaxation mechanism is attributed to β-relaxation this may be due to the orientation of the side chains and/or attached groups in the polymer. Clearly, the semicircles nature changed by incorporating Fe_3O_4 as depicted by the changes of the semicircles radius. This means that the relaxation mechanisms are affected by its incorporation. Moreover, the semicircle nature reduced and becomes more skewed at higher Fe_3O_4 content. The start of semicircles matched with the graph origin is a definite sign that no supplementary relaxation process is existed at lower frequencies in all investigated concentrations.

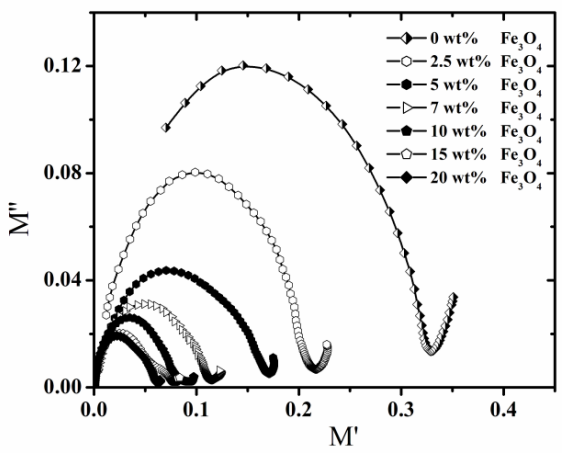

Figure (4): Cole–Cole plots of M" vs. M' for PVA doped with Fe_3O_4 at RT.

Figure (5) depicts the change of AC conductivity with frequency for various Fe_3O_4 loading in PVA. According to the graph, for all loading conductivity rises as both frequency and content of Fe_3O_4 increases following power law function;

$\sigma = A\,\omega^s$……. Eq (1)

Where ω is angular frequency, A is a parameter independent upon the frequency whiles is a power value and are found to be $s \leq 1$, it is governed by the electronic hopping processes [23,24]. It was discovered that the ac conductivity at room temperature remained constant. Conductivity rises regardless of frequency at low and high frequencies [25]. The electronic and ionic mobility rises as the concentration of Fe_3O_4 increases. As a result, as the hopping electron charge carrier interacts with the defects produced in the polymer chain, the conductivity rises [26]. DC conductivity σ_{dc} was calculated from power law fitting as declared in Figure (5) a and the obtained values are presented in Figure (5) b. The observer could clearly see that σ_{dc} values increases pronouncedly after 10 wt% loading of Fe_3O_4. From the dielectric as well as conductivity data it is concluded that 10 wt% loading of Fe_3O_4 is the much more promising composite for further investigations. For this reason $BaTiO_3$ in various concentrations was doped with host PVA / 10wt% Fe_3O_4 matrix to form ternary PVA composite for enhancing the electrical / magnetic properties.

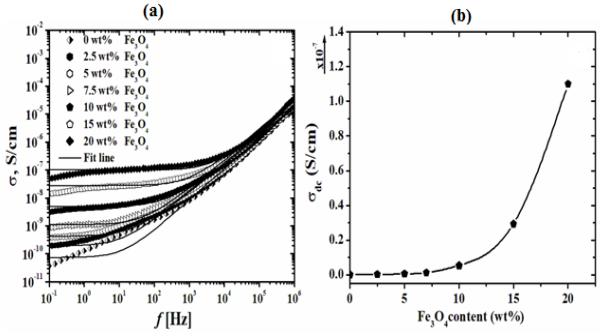

Figure (5): (a) σ vs. *f* for PVA doped with different Fe_3O_4 loadings at RT. The fit lines in according to power law Eq. (1). (b)Variation of DC conductivity with Fe_3O_4 content.

The effect of various concentrations of $BaTiO_3$ on real part of ε′ and ε″ in the frequency range (10^{-1} – 10^6 Hz) and their respective graphs are given in the Fig.6. ε′ measures the energy stored while ε″ is a measure of energy dissipated due to molecular collisions as the composite dipoles do work and lag for aligning themselves parallel to the applied electric field [27]. At low frequency, it is notable that both ε′ and ε″ are high, this is because of the charge polarization close to the electrode – electrolyte border due to the free mobile charges in the back bone of PVA [28-30]. The increase in ε′ with increasing $BaTiO_3$ loading is related to the fact that micro-capacitors are constructed by particles near to each other and ultra-thin PVA separated in the centre under electric field [31-33]. Both ε′ and ε″ decreases by increasing *f*, this is because of fact that the dipoles of composite molecules are not capable to rotate parallel with respect to speedy periodic phase turnaround of electric field and the result is time lag between the frequency of dipole and that of electric field [34], this finding means that there is no ion dissemination and charge build up. As seen in Figure (6), the ε″ of the NCPs reduced fast at low *f* values and subsequently increased somewhat at high *f* as the testing frequency increased. The increase in $BaTiO_3$ concentration resulted in a significant rise in ε″ of the NCPs at low *f*, which was attributed to the high leakage conductance [35] caused by the PVA /

$BaTiO_3$ interface areas. At higher *f*, the values of ε″ for all NCPs changed slightly and remained low. Figure (6) b illustrates the relationship between both ε′ and ε″ and $BaTiO_3$ loading in the nanocomposites. The general trend noticed was the abrupt increase in both values after 10% of $BaTiO_3$. This finding suggests that concentration to be the most promising one for energy storage applications.

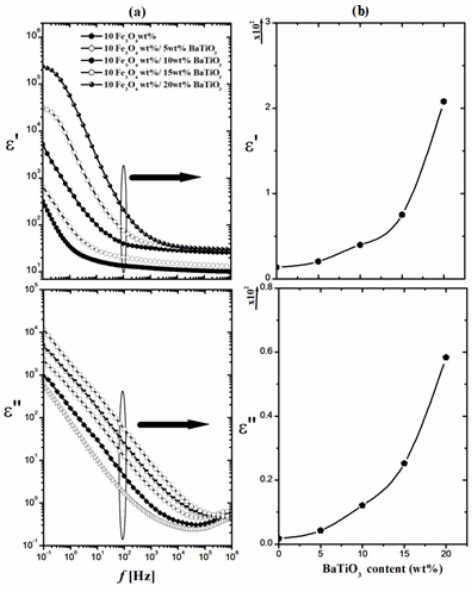

Figure (6): (a) ε′ and the ε″ *vs f* for PVA / 10 wt% Fe_3O_4 / $BaTiO_3$ nanocomposites and both values versus $BaTiO_3$ at fixed *f* = 100 Hz presented in (b) at RT.

The Nyquist diagram in Figure (7) shows the electric modulus complex plane plots (Cole–Cole plots) drawn as M'' vs. M' (imaginary part of electric modulus vs. real part of electric modulus) for PVA / 10 wt% Fe_3O_4 / $BaTiO_3$ nanocomposites. As in Figure (4), the Cole–Cole plots disclose two arcs corresponding to αβ and β-relaxation respectively. The semicircle radius influenced by incorporating $BaTiO_3$ and becomes more skewed at than those in Figure (4). This a clear sign that the relaxation mechanisms are affected by $BaTiO_3$ incorporation.

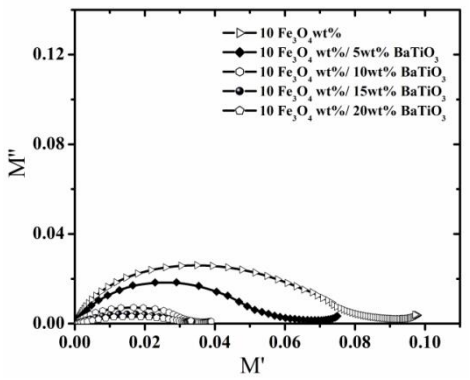

Figure (7): M'' vs. M' (imaginary part of electric modulus vs. real part of electric modulus) for PVA / 10 wt% Fe_3O_4 / $BaTiO_3$ nanocomposites at RT.

Figure (8) a, presents the variation of σ vs. frequency *f* for PVA / 10 wt% Fe_3O_4 doped with different $BaTiO_3$ loadings at RT. At low ***f***, conductivity of all NCPs was kept at low levels, indicating low border leakage conduction in composite system [36]. At high ***f***, σ values increase. As the concentration of $BaTiO_3$ increases, the electronic and ionic mobility increases. So the conductivity increases as hopping electron charge carrier interacts with the defects formed in PVA chain [26]. DC conductivity σ_{dc} was calculated as explained previously and illustrated versus $BaTiO_3$

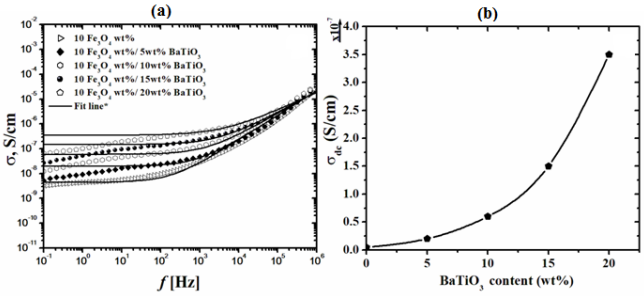

in Figure (8) b. The observer could clearly see that σ_{dc} values increases pronouncedly or with loading of $BaTiO_3$.

Figure (8): (a) σ vs. *f* for PVA / 10 wt% Fe_3O_4 doped with different $BaTiO_3$ loadings (b) Variation of DC conductivity with $BaTiO_3$ content at RT.

However the effect of $BaTiO_3$ treatment with ionic liquid as mentioned before were also investigated [9]. In this investigation 10wt% Fe_3O_4 was added to the various content of treated $BaTiO_3$ to form hybrid nanocomposites. The obtained dielectric data are presented in Figure (9). Further increase in both ε′ and ε″ was detected after IL treatment see Figure (9). The permittivity ε′ of hybrid NCP contain IL treated $BaTiO_3$ are significantly greater than that of untreated ones Figure (6). The increase in ε′ with increasing IL treated $BaTiO_3$ content is related to the construction of the micro-capacitors by particles near to each other and ultra-thin PVA separated in the centre under electric field [37,38]. In addition, the increase in ε′ values for NCPs containing IL treated $BaTiO_3$ when compared with those untreated Figure (6) is attributed to the presence of the low molecular weight ionic liquid which is characterized by its high ε′. This ionic liquid physically interacts with PVA and the result is decrease in the viscosity and consequently forms higher number of charge carriers [39]. Figure (9) shows also the variation of ε″ versus the frequency. Values of ε″ are directly correlated to the relaxation phenomenon of composites and considered to be the events of the exponential decay of polarization with respect to time [19]. It is also seen that the ε″ values of the NCPs increased fast at low frequencies and subsequently reduced somewhat at high frequencies as the testing frequency increased. The increase in IL treated $BaTiO_3$ content resulted in a significant rise in ε″ values of the nano composites at low frequencies, which was attributed to the high leakage conductance caused by the hybrid NCPs interface areas. The ε″ values reduced quicker in the NCPs with increasing IL treated $BaTiO_3$ percentage in the low frequency range of 10^{-1}–10^3 Hz. The comparatively high ε″ values of the hybrid NCPs at low frequencies should be attributed to the impeded orientation of ionic dipoles in it as a result of a strong coupling effect between the high-polarity ionic dipoles due to the presence of ionic liquid [17]. At 10^4–10^7 Hz, the ε″ values of all NCPs changed slightly. Overall, the ε″ values of hybrid NCP contain IL treated $BaTiO_3$ are significantly greater than that of untreated ones. At a 10 wt% loading ε″of the film contain $BaTiO_3$ before treatment was about 40 at 100 Hz but it can reach up to 100 at the same frequency for NCP containing 10 wt% of IL treated $BaTiO_3$, approximately two times greater than the untreated one. This finding suggests such composite to be our optimum concentration recommended for energy storage applications.

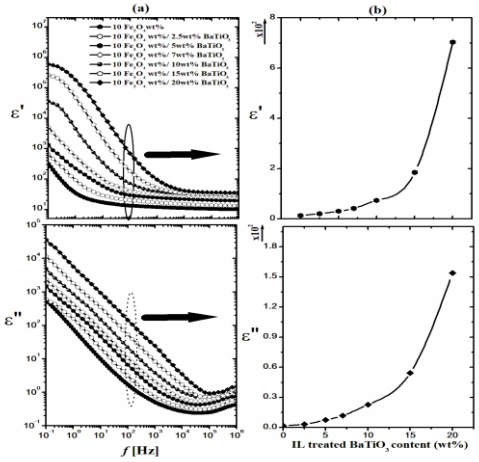

Figure (9): (a) ε′ and ε″ versus f for PVA / 10 wt% Fe_3O_4 / IL treated $BaTiO_3$ and (b) both values versus IL treated $BaTiO_3$ at fixed f = 100 Hz at RT.

Surprisingly the addition of untreated and IL treated $BaTiO_3$ to PVA / 10wt% Fe_3O_4 has a good impact on loss factor tanδ as shown in Figure (10) as it decreased upon increasing the loading of both of them. These finding suggest these composites to be recommended for high k applications.

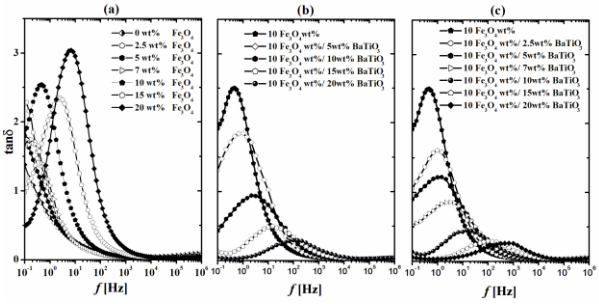

Figure (10): The loss factor tanδ at RT versus frequency for f for the three investigated systems.

On the other hand Figure (11) a, presents the variation of σ vs. frequency f for PVA /10 wt% Fe_3O_4 doped with different IL treated $BaTiO_3$ loadings at RT. From which σ_{dc} was calculated as mentioned above and given in Figure (11) b. From this figure it is clear that the values of σ_{dc} lies in the order of 10^{-7} S/cm this finding highly recommend such NCPs to be used as anti dissipation composites as the demanded range for such application was 10^{-5} –10^{-9} S/cm [40].

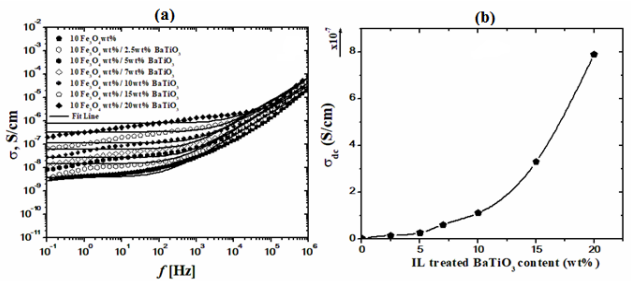

Figure (11): (a) σ vs. *f* for PVA / 10 wt% Fe_3O_4 doped with different IL treated $BaTiO_3$ loadings at room temperature. (b) Variation of DC conductivity with IL treated $BaTiO_3$ content at RT.

5. Conclusion

All composites under investigations were prepared by using casting technique. Magnetic investigations led to the conclusion that the presence of ionic liquid in the nanocomposites improved the magnetic properties which recommend such composites to be used in many electromagnetic applications. The permittivity ε′and dielectric loss ε″ values of composites are found to be the optimum in case of Fe_3O_4 and treated $BaTiO_3$ with ionic liquid particles.
The percolation threshold is defined as the stage that electrical conductivity reaches the values 10^{-7} S/cm. In fact the highest values of the σ_{dc} values were detected in case of IL treated $BaTiO_3$ / Fe_3O_4 composites. This finding recommend the using of such composites for electrostatic dissipation applications because the range needed for such application is 10^{-5}–10^{-9} S/ cm.

6. Acknowledgment

The authors also Acknowledge the in-house projects in National Research Centre, Dokki, Giza, Egypt for funding support of this work through the in-house project no 12020225.

7. References

1. AbasianMojtaba, VahidHooshangi, and PeymanNajafiMoghadam. "Synthesis of polyvinyl alcohol hydrogel grafted by modified Fe_3O_4 nanoparticles: characterization and doxorubicin delivery studies." Iranian Polymer Journal 26, no. 5 (2017): 313-322.
2. Usawattanakul, Naphat, SelormTorgbo, PrakitSukyai, SomwangKhantayanuwong, BuapanPuangsin, and PreeyanuchSrichola. "Development of Nanocomposite Film Comprising of Polyvinyl Alcohol (PVA) Incorporated with Bacterial Cellulose Nanocrystals and Magnetite Nanoparticles." *Polymers* 13, no. 11 (2021): 1778.
3. Wang, Ya Jun, and Xiao Juan Wu. "Preparation of barium titanate/polyimide composite film and its dielectric properties." In Advanced Materials Research, vol. 815, pp. 93-98. Trans Tech Publications Ltd, (2013).
4. Wilk, Glen D., Robert M. Wallace, and JáM Anthony. "High-κ gate dielectrics: Current status and materials properties considerations." *Journal of applied physics* 89, no. 10 (2001): 5243-5275.
5. Pratap, A., N. J. Joshi, P. B. Rakshit, G. S. Grewal, and V. Shrinet. "Dielectric behavior of nano barium titanate filled polymeric composites." In International Journal of Modern Physics: Conference Series, vol. 22, pp. 1-10. World Scientific Publishing Company, (2013).
6. Deng, Qihuang, Junquan Zhou, Xianping Li, YefengFeng, Yurun Liang, and Qihang Liu. "Finely-reconciled high dielectric constant and low dielectric loss in ternary polymer/Cr_2C_3/montmorillonite composite films by filler-synergy strategy." Current Applied Physics 22 (2021): 104-110.
7. Mjakin, Sergey, Maxim Sychov, AndreyChekuryaev, and NikolaySudar. "Adjustment of dielectric performances for polymer-inorganic composites by ferroelectric filler modification with graphene micro-additive." Materials Today: Proceedings 30 (2020): 603-605.
8. Adel, D., A. A. Ward, N. Lotfy, A. Nassar, S. L. Abd-El-Messieh, M. A. Hafez, and Y. A. Badr. "PMMA nanocomposites based on laser fragmented Fe_3O_4 nanoparticles." KGK-KAUTSCHUK GUMMI KUNSTSTOFFE 70, no. 9 (2017): 32-38.
9. D. A. Wissa, N. N. Rozik, S. A. Gad, A. A. Ward, S. S. Ibrahim, A. Nassar, S. L. Abd-El-Messieh, Sh. A. Khairy, "Novel Polyvinyl Alcohol/Barium Titanate Nanocomposites Modified by Ionic Liquid", KGK-KAUTSCHUK GUMMI KUNSTSTOFFE (2022) Accepted.
10. Villa, Sara Moon, Vittorio Massimo Mazzola, TommasoSantaniello, Erica Locatelli, MirkoMaturi, Lorenzo Migliorini, Ilaria Monaco, Cristina Lenardi, Mauro Comes Franchini, and Paolo Milani. "Soft piezoionic/piezoelectric nanocomposites based on ionogel/$BaTiO_3$ nanoparticles for low frequency and directional discriminative

pressure sensing." ACS Macro Letters 8, no. 4 (2019): 414-420.
11. Jayakrishnan, P., and M. T. Ramesan. "Synthesis, characterization, electrical conductivity and material properties of magnetite/polyindole/poly (vinyl alcohol) blend nanocomposites." Journal of Inorganic and Organometallic Polymers and Materials 27, no. 1 (2017): 323-333.
12. Zhang, Yu-Ping, Se-Hee Lee, KakarlaRaghava Reddy, AnanthaIyengarGopalan, and Kwang-Pill Lee. "Synthesis and characterization of core-shell SiO_2 nanoparticles/poly (3-aminophenylboronic acid) composites." Journal of Applied Polymer Science 104, no. 4 (2007): 2743-2750.
13. Jacobo, Silvia E., Juan C. Aphesteguy, R. Lopez Anton, N. N. Schegoleva, and G. V. Kurlyandskaya. "Influence of the preparation procedure on the properties of polyaniline based magnetic composites." European Polymer Journal 43, no. 4 (2007): 1333-1346.
14. Mikhaylova, Maria, Do Kyung Kim, Natalia Bobrysheva, Mikhail Osmolowsky, Valentin Semenov, Thomas Tsakalakos, and MamounMuhammed. "Superparamagnetism of magnetite nanoparticles: dependence on surface modification." Langmuir 20, no. 6 (2004): 2472-2477.
15. Bhatt, Aarti S., D. Krishna Bhat, and M. S. Santosh. "Electrical and magnetic properties of chitosan-magnetite nanocomposites." Physica B: Condensed Matter 405, no. 8 (2010): 2078-2082.
16. Badawy, Sayed M., and A. A. Abd El-Latif. "Synthesis and characterizations of magnetite nanocomposite films for radiation shielding." Polymer Composites 38, no. 5 (2017): 974-980.
17. Feng, Yefeng, Junquan Zhou, Peiyao Chen, Maolin Bo, and Qihuang Deng. "Filler-synergy route for optimising dielectric features of novel polymer-based ternary composite films bearing Fe_2TiO_5 pseudo-perovskite and graphite particles." Ceramics International 47, no. 6 (2021): 8357-8364.
18. Iwauchi, Kōzō, Shigehisa Yamamoto, Yoshichika Bando, Tetsuya Hanai, Naokazu Koizumi, Toshio Takada, and Syōji Fukushima. "Dielectric Properties of the Mixtures of α-Fe_2O_3, TiO_2 and Fe_2TiO_5." Japanese Journal of Applied Physics 10, no. 11 (1971): 1513.
19. Ravikumar, K., K. Palanivelu, and K. Ravichandran. "Dielectric properties of natural rubber composites filled with graphite." Materials Today: Proceedings 16 (2019): 1338-1343.
20. Abd-El Messieh, Salwa L., Nehad N. Rozik, and Nadia F. Youssef. "Eco-friendly composites based on ceramic tiles industrial wastes and acrylonitrile butadiene rubber." Polymer Composites 40, no. 2 (2019): 544-552.
21. Ward, A. A., S. L. Abd-El-Messieh, A. I. Khalaf, and D. A. El Nashar. "Use of natural Oils as potential Additives in filled Rubber Compounds for antistatic Applications." KGK KautschukGummiKunststoffe 72 (2019): 36-44.
22. Thakur, Yash, Rui Dong, Minren Lin, Shan Wu, Zhaoxi Cheng, Ying Hou, J. Bernholc, and Q. M. Zhang. "Optimizing nanostructure to achieve high dielectric response with low loss in strongly dipolar polymers." Nano Energy 16 (2015): 227-234.
23. Beena, P., R. K. Raju, and H. S. Jayanna. "AC conductivity and dielectric behaviour of $NaNbO_3$ ceramic polymer composites." Materials Today: Proceedings 37 (2021): 1973-1977.
24. Venkataraman, B. H., and K. B. R. Varma. "Microstructural, dielectric, impedance and electric modulus studies on vanadium—doped and pure strontium bismuth niobate ($SrBi_2Nb_2O_9$) ceramics." Journal of Materials Science: Materials in Electronics 16, no. 6 (2005): 335-344.
25. More, S. S., R. J. Dhokane, and S. V. Mohril. "Study on structural characterization and dielectric properties of PVA–TiO_2 composite." IOSR J ApplPhys 8 (2016): 28-32.
26. Al-Akhras, M. A., S. Saq'an, and Z. Ghadieh. "Ac Electrical Properties of Polystyrene / Ferroelectric Barium StannateTitanate Ba (Ti0. 9 Sn0. 1) O_3 Ceramic Composite." ActaPhysicaPolonica A 130, no. 1 (2016): 447-449.
27. Choudhary, Shobhna, and R. J. Sengwa. "Dielectric properties and structural conformation of melt compounded PEO-$LiCF_3SO_3$-MMT nanocomposite electrolytes." Indian J. Pure Appl. Phys. 49 (2011) 602–605.
28. Pradhan, Dillip K., R. N. P. Choudhary, and B. K. Samantaray. "Studies of dielectric relaxation and AC conductivity behavior of plasticized polymer nanocomposite electrolytes." Int. J. Electrochem. Sci 3, no. 5 (2008): 597-608.

29. Campbell, Jonathan A., Andrew A. Goodwin, and George P. Simon. " Dielectric relaxation studies of miscible polycarbonate / polyester blends." Polymer 42, no. 10 (2001): 4731-4741.
30. Sangeetha, M., A. Mallikarjun, Y. Aparna, M. Vikranth Reddy, J. Siva Kumar, T. Sreekanth, and M. Jaipal Reddy. "Dielectric studies and AC conductivity of PVDF-HFP: LiBF4: EC plasticized polymer electrolytes." Materials Today: Proceedings 44 (2021): 2168-2172.
31. Wu, Weifei, Xueqing Liu, ZheQiang, Jiying Yang, Yuhong Liu, Kai Huai, Bailang Zhang et al. "Inserting insulating barriers into conductive particle channels: A new paradigm for fabricating polymer composites with high dielectric permittivity and low dielectric loss." Composites Science and Technology 216 (2021): 109070.
32. Guo, Yuanhao, Yuwei Chen, Enmin Wang, and Miko Cakmak. " Roll-to-roll continuous manufacturing multifunctional nanocomposites by electric - field - assisted "Z" direction alignment of graphite flakes in poly(dimethylsiloxane). "ACS applied materials & interfaces 9, no. 1 (2017): 919-929.
33. Chen, Yuwei, Yuhong Liu, Jiying Yang, Bailang Zhang, Zhendong Hu, Quan Wang, Weifei Wu et al. "Fabrication of high dielectric permittivity polymer composites by architecting aligned micro-enhanced-zones of ultralow content graphene using electric fields." Materials Today Communications 21 (2019): 100649.
34. Naik, Jagadish, R. F. Bhajantri, Sunil G. Rathod, T. Sheela, and V. Ravindrachary. "Synthesis and characterization of multifunctional ZnBr2/PVA polymer dielectrics." Journal of Advanced Dielectrics 6, no. 04 (2016): 1650028.
35. Deng, Qihuang, Xiaoxiao Li, Qin Li, Xiaofeng Xia, YefengFeng, and Cheng Peng. "Well-balanced high permittivity and low dielectric loss obtained in PVDF/graphite/BN ternary composites by depressing interfacial leakage conduction." Microelectronic Engineering 231 (2020): 111404.
36. Deng, Qihuang, Furong Zhou, Maolin Bo, YefengFeng, Yuehao Huang, and Cheng Peng. "Remarkably improving dielectric response of polymer/hybrid ceramic composites based on 0D/2D-stacked CuO/V_2C MXeneheterojunction." Applied Surface Science 545 (2021): 149008.
37. Wu, Weifei, Xueqing Liu, ZheQiang, Jiying Yang, Yuhong Liu, Kai Huai, Bailang Zhang et al. "Inserting insulating barriers into conductive particle channels: A new paradigm for fabricating polymer composites with high dielectric permittivity and low dielectric loss." Composites Science and Technology 216 (2021): 109070.
38. Chen, Yuwei, Yuhong Liu, Jiying Yang, Bailang Zhang, Zhendong Hu, Quan Wang, Weifei Wu et al. "Fabrication of high dielectric permittivity polymer composites by architecting aligned micro-enhanced-zones of ultralow content graphene using electric fields." Materials Today Communications 21 (2019): 100649.
39. Sangeetha, M., A. Mallikarjun, Y. Aparna, M. Vikranth Reddy, J. Siva Kumar, T. Sreekanth, and M. Jaipal Reddy. "Dielectric studies and AC conductivity of PVDF-HFP: $LiBF_4$: EC plasticized polymer electrolytes." Materials Today: Proceedings 44 (2021): 2168-2172.
40. Huang, Jan-Chan. "Carbon black filled conducting polymers and polymer blends." Advances in Polymer Technology: Journal of the Polymer Processing Institute 21, no. 4 (2002): 299-313.